Pergamon

Journal of Structural Geology, Vol. 17, No. 12, pp. 1741 to 1755, 1995
Elsevier Science Ltd
Printed in Great Britain
0191-8141/95 $9.50+0.00

0191-8141(95)00071-2

Relay zone geometry and displacement transfer between normal faults recorded in coal-mine plans

P. HUGGINS, J. WATTERSON, J. J. WALSH and C. CHILDS

Fault Analysis Group, Department of Earth Sciences, University of Liverpool, P.O. Box 147, Liverpool L69 3BX, U.K.

(*Received* 3 *August* 1994; *accepted in revised form* 19 *June* 1995)

Abstract—Overlap lengths, separations and throw gradients were measured on 132 relay zones recorded on coal-mine plans. Throws on the relay-bounding fault traces are usually ≤2 m and individual structures are recorded on only one seam. Throw gradients associated with relay zones are not always higher than on single faults, but asymmetry of throw profiles is diagnostic of relay zones. Bed geometries around larger faults in open-cast mines are used to assess the displacement accommodated by shear in the vertical plane normal to the faults and displacement transfer accommodated by shear in the fault-parallel plane. Three-dimensional structure is defined for two relay zones, each recorded on five seam plans. These relay zones are effectively holes through the fault surfaces and overlap occurs between salients or lobes of the parent fault surfaces. Lobes initially terminated at tip-lines but, as the faults grew, gradually rejoined the main fault surfaces along branch lines. This type of relay zone originates by bifurcation of a single fault surface at a locally retarded tip-line and is an almost inevitable result of a tip-line irregularity.

INTRODUCTION

Relay zones are a special case of fault overlap and occur on a wide range of scales; their complex, three-dimensional geometries change throughout fault growth. The term *overlap zone* refers either to a two-dimensional, geometrical relationship between two fault traces, or to the corresponding three-dimensional structure (Childs *et al.* 1995), but implies no specific mechanical or kinematic relationship between the faults. If the faults bounding the overlap zone dip in the same direction and are demonstrated to have interacted kinematically, the rock volume of the overlap zone is referred to as a *relay zone* and, in sub-horizontally layered rocks, will contain a *relay ramp* (Larsen 1988). Two faults are considered to have interacted kinematically if there are complementary modifications of their displacement patterns and if associated horizon geometries indicate displacement transfer (Muraoka & Kamata 1983, Larsen 1988, Walsh & Watterson 1990, Peacock & Sanderson 1994). Displacement geometries and displacement gradients of single isolated faults (Walsh & Watterson 1987, 1989, Dawers *et al.* 1993) are a reference standard for identification of variants. All the overlap zones identified in this study are relay zones and are referred to as such.

The systematics of fault segmentation and relay zones are relevant to the growth and scaling properties of single faults and fault arrays (Gillespie *et al.* 1992, Cowie & Scholz 1992 a,b, Cartwright *et al.* 1995) and also to the hydrocarbon trapping potential of faults (Larsen 1988, Morley *et al.* 1990, Woods 1992, Peacock & Sanderson 1994, Childs *et al.* 1995). Relay zones between coeval faults may be either 'incidental', formed by growth towards one another of two independently nucleated faults (e.g. Morley *et al.* 1990) or may form by out-of-plane bifurcation of a single fault surface, or by upward propagation of several fault segments from a single basement fault (Larsen 1988, Childs *et al.* 1995). However, as most relay zones are identified on two-dimensional maps or sections, the three-dimensional structure is usually unknown.

An observed relay zone geometry represents only one stage in the evolution of a structure which initiates, grows and, unless growth ceases, is likely to be breached. The internal structure of a relay zone will vary according to its origin and the stage at which fault growth ceases. The former existence of a relay zone along a now continuous fault trace can be demonstrated in some cases (Childs *et al.* 1995), but general rules for identifying breached relay zones have not been defined. The rules governing each growth stage of relay zones need to be established and methods developed for distinguishing between relay zones formed in different ways.

Relay zones occur on a wide range of scales (Stewart & Hancock 1991, Peacock & Sanderson 1994) but their scaling relationships are not known. No single data type is ideal for studying relay zones over their full scale range, so a variety of data types is necessary. This paper is based on one type of data and addresses three topics: (i) the two-dimensional systematics of a sample of small relay zones (throws on bounding faults ≤2 m), (ii) the two-dimensional internal structure of larger relays (throws ≤25 m); and (iii) the three-dimensional structure of two small relay zones, each recorded on five seams.

DATA

Data sources

The data include 1:2500 *seam abandonment plans* from deep mines, which are drawn up when extraction

from a U.K. coal seam has ceased. The plans are mainly from the East Pennine Coalfield, with some from the Lancashire and Staffordshire Coalfields. The smallest fault throws recorded on seam plans are ca. 15 cm, or 6 in., so a fault trace may continue for tens of metres beyond the mapped tip-point (Walsh & Watterson 1987, Watterson *et al.*, in press). Each abandonment plan is of a 2 × 1 km area so relay zones with map dimensions of more than ca. 500 m are rarely identified; this size limit has no geological significance but imposes an upper limit of ca. 2.0 m on the throw of the relay bounding faults. Most relay structures are recorded only on one seam but in two cases relay structures are recorded on five seams, allowing their three-dimensional geometries to be determined. In addition to the small relay zones recorded in deep-mine data, some larger structures have been studied, which are recorded on plans from open-cast coal operations.

The faults included in the database are predominantly tectonic normal faults; data from strike-slip and soft-sediment faults, which also occur, have been excluded where positive identification was possible. The emphasis on map views of normal fault overlap zones means that the fault trace tip-points are predominantly of Mode III type, i.e. those comparable with screw dislocations. Our results are therefore not directly comparable with those obtained from map analyses of strike-slip faults (Aydin & Nur 1982, Aydin & Schultz 1990), where the fault trace tip-points are predominantly of Mode II type and comparable with edge dislocations.

Data collation—1:2500 underground seam plans

Overlap zones were identified on purely geometrical criteria which included: (i) the two overlapping fault traces having similar strike directions; and (ii) the overlap zone, being sufficiently distant from other faults to be an effectively isolated structure. This second condition is considered to be met where no other fault of comparable size is closer than a strike-normal distance equivalent to one-half of the trace length of the longer of the two traces forming the overlap zone. Where fault traces overlap for more than half the trace length of one of the constituent faults, the relationship is regarded as one between 'parallel' rather than overlapping faults, and the data are not included in the database. Where the strike-normal distance between two fault traces is greater than one-half of the trace length of either, the faults are regarded as isolated, rather than overlapping. Identification of overlap zones is, therefore, to some degree both arbitrary and subjective. One hundred and thirty-two synthetic overlap zones (both faults dipping in the same direction) were identified; in seven cases, the overlapping faults are joined by linking faults and, in 18 cases, the structures underlap, i.e. with en bayonet rather than en échelon structure.

The parameters which characterize overlap zones are shown in Fig. 1; each of these parameters, together with fault trace lengths and throw maxima, was recorded where possible. Throw gradients are calculated as linear

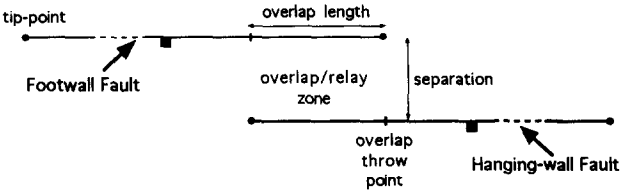

Fig. 1. Schematic map view of a relay zone between two fault trace segments, showing the main parameters recorded for the relay zones studied.

gradients between adjacent throw readings on a fault trace; where only one throw reading is shown on a fault trace, it is assumed to be the maximum throw on that trace. Throw gradients in overlap zones were measured as the gradient between the overlap point (Fig. 1) and the tip-point on each fault trace: allowance was made for the limited resolution of the data by assigning throws of 0.15 m to mapped tip-points. Throw gradients are subject to significant error (up to a factor of ca. 2) and are best regarded as minimum estimates. The two faults which bound an overlap zone are referred to as the footwall and hangingwall faults depending on their relative positions (Fig. 1).

TWO-DIMENSIONAL CHARACTERISTICS

Relay zones are mostly identified on only one seam, either because data are not available for other seams, or because either the fault or the overlap zone dies out within the interval between seams. The relay zones are usually simple, parallel-sided structures, but in some cases the fault trace tips are deflected with geometries similar to those described for en échelon cracks (Segall & Pollard 1980) and fracture tip deflections in joints, veins and dikes (Delaney & Pollard 1981, Rogers & Bird 1987, Cruikshank *et al.* 1991). There are relatively few examples of two or more relay zones within a single fault array, and of the 24 examples of multiple relay zones identified, 19 show a consistent sense of offset.

Throw profiles

A throw profile (Fig. 2) shows the throw distribution along a line on a fault surface; the examples shown are along fault traces on a map, i.e. approximately normal to the slip direction of a normal fault. The standard profile is a bell-shaped curve (Walsh & Watterson 1987), but both shape and throw gradients may vary with the position of a profile with respect to the centre of the fault surface. Abrupt changes in gradient may occur where a profile crosses a lithological boundary (Muraoka & Kamata 1983) but such boundaries do not occur on seam plans. On seam plans, abrupt changes in throw gradient, or unusually high gradients, are likely to be due to displacement transfer between neighbouring faults (Walsh & Watterson 1990).

Figure 2 shows throw profiles associated with relay zones in the coalfield data. Where data are available for

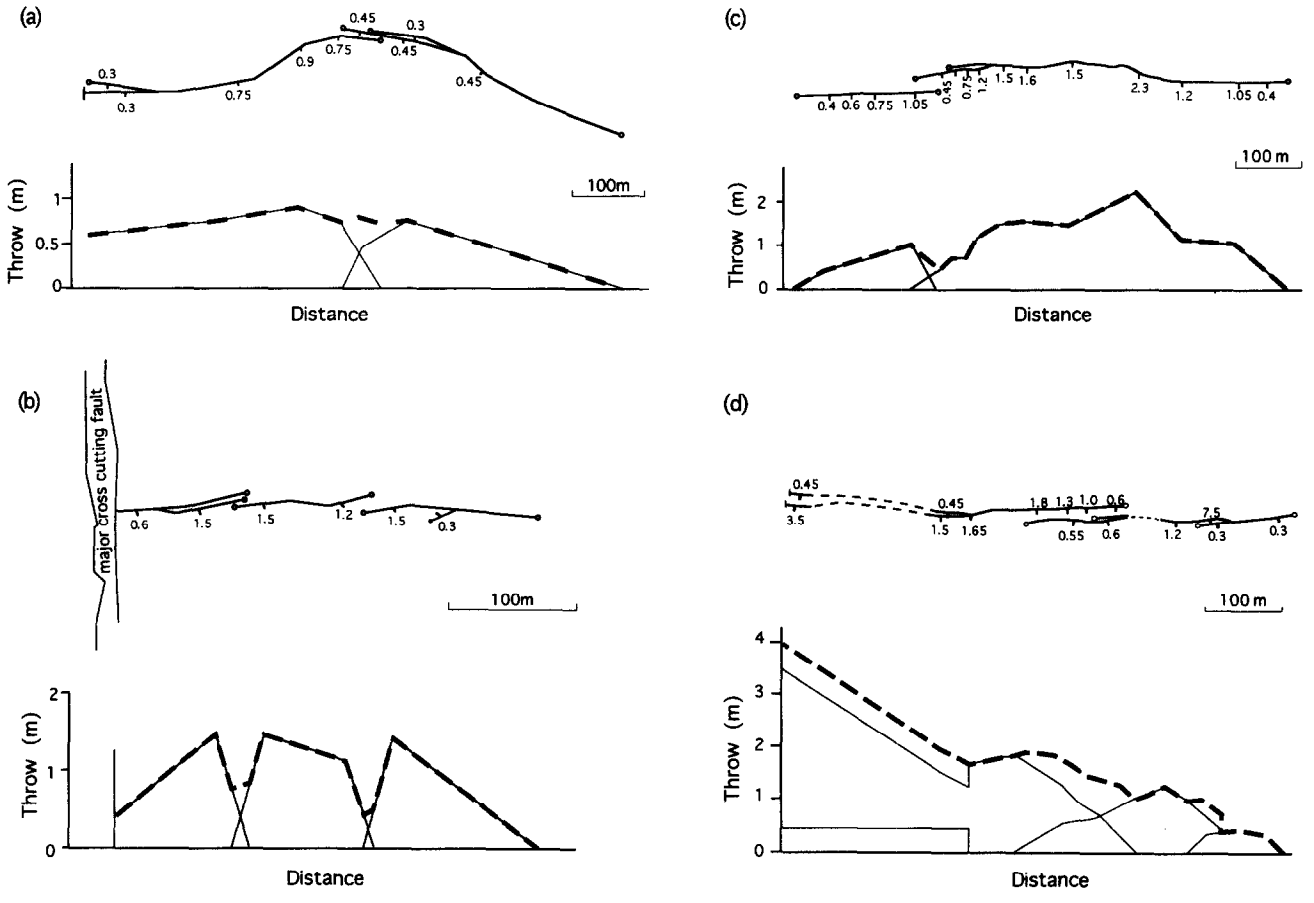

Fig. 2. Fault trace geometries and corresponding throw profiles for four segmented faults. Recorded throw values (m), fault throw directions (tick on downthrown side), fault trace tip-points (open circles), and ends of data (vertical bars) are shown. Throw profiles show individual trace profiles (thin solid lines) and aggregate throw profiles (thick broken lines). (a) Silkstone seam, Rockingham Colliery, South Yorkshire; (b) Parkgate seam, Denaby Main Colliery, South Yorkshire; (c) 1st Waterloo seam, Glapwell Colliery, Derbyshire—note that throw readings on the footwall splay were not recorded; (d) 2nd Waterloo seam, Silverwood Colliery, South Yorkshire.

the entire lengths of the individual fault traces, the throw profiles vary from symmetric to strongly asymmetric in form (Fig. 2). Symmetrical profiles with steep throw gradients are characteristic of the central segments of en échelon arrays, and asymmetrical profiles characteristic of end segments (Fig. 2b). Asymmetry of throw profiles along individual fault traces and steepening of throw gradients within a relay zone are reliable indications of fault interaction. Throw profiles on overlapping fault trace pairs are complementary and when the throws on the individual faults are summed in the extension direction, they provide aggregate profiles of throw (Figs. 2a, b & d) which are similar to those typical of continuous single fault traces (Muraoka & Kamata 1983, Walsh & Watterson 1989, 1990, Dawers *et al.* 1993, Scholz *et al.* 1993).

Overlapping fault traces may have an aggregate throw profile showing a throw 'low' coincident with the relay zone (Figs. 2c and 3). Where there is no throw reading on a trace within a relay zone, the assumption of a linear displacement profile to a fault tip may produce a low aggregate throw which is not real (Fig. 2b). A real decrease in aggregate throw across a relay zone could occur if it developed by interaction of independently nucleated faults (Peacock & Sanderson 1991), and/or if a significant proportion of displacement is accommodated by ductile strain within the relay zone. Although throw profiles of incidental overlap zones may sometimes be distinctive, they will often not be distinguishable from those of non-incidental overlap zones. As the relay zones we have examined are spatially isolated from other faults and occur in areas of low fault density, we believe that most of the relay zones identified are not incidental structures and that decreases in aggregate throws are due to significant displacement being accommodated by ductile strain within relay zones. This ductile (or continuous) displacement, as opposed to discontinuous displacement along a discrete fault surface, is accommodated by strain within the relay volume, in the form of folding or sub-resolution faulting (Peacock & Sanderson 1994, Walsh *et al.* 1995) or normal 'fault drag' (Rippon 1985). As the throw component accommodated by normal drag is often not included in the recorded throw values (Rippon 1985, Walsh & Watterson 1987), some low aggregate throw values may be due to normal drag. Figure 3 shows an exceptional example where increased normal drag adjacent to a relay zone, as shown by the depth contours, is compensated for by a decrease in the discontinuous component of throw. Structure contour data are available for only a few relay zones

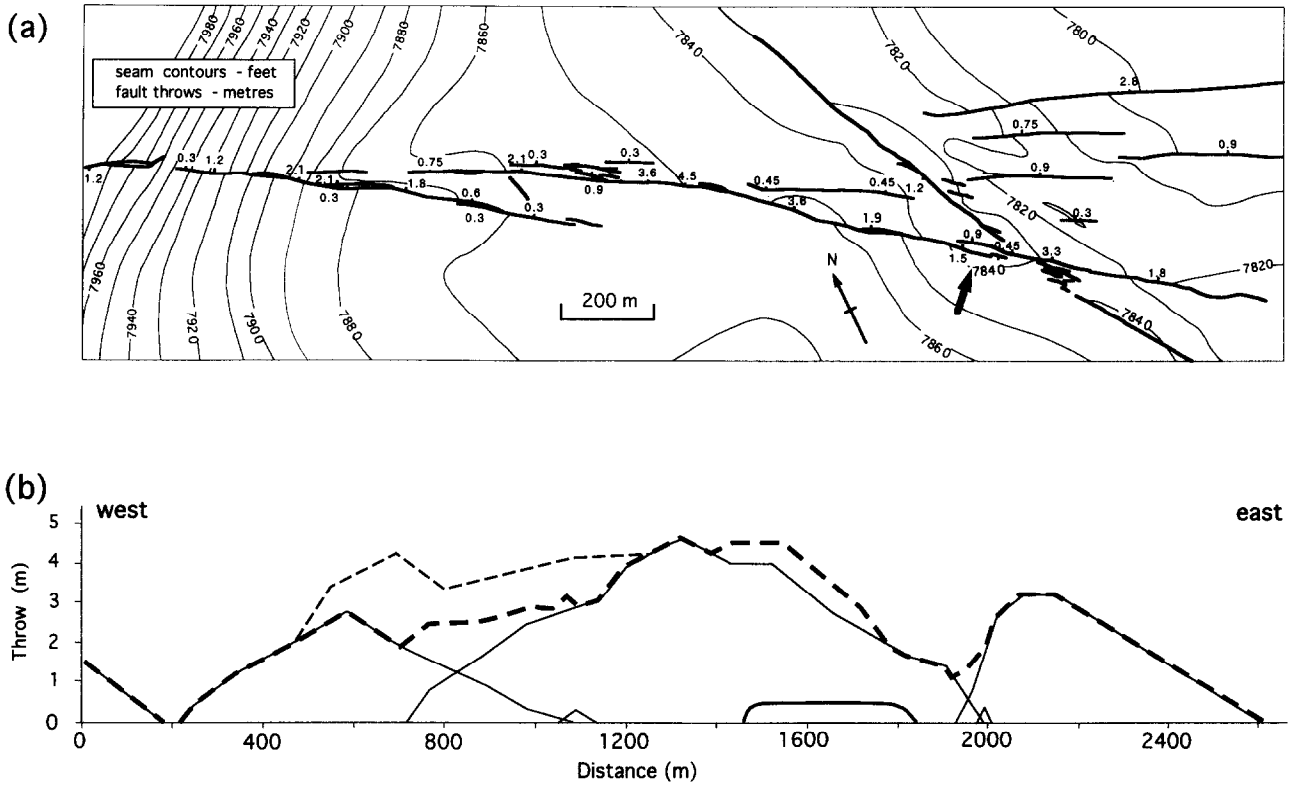

Fig. 3. Trace geometries and throw profiles for a segmented fault, Barnsley seam, Silverwood Colliery, South Yorkshire. (a) Fault trace map (heavy solid lines) with recorded fault throw values (m) and fault throw directions (ticks on downthrown sides). Seam contours (feet above datum at 10,000 ft below sea level) are shown as light solid lines; (b) throw profiles along the four main traces of the segmented fault (thin solid lines), aggregate throw profile (heavy broken line) and total throw profile including the throw component due to normal drag in the main overlap zone (thin dashed line). Normal drag adjacent to the eastern overlap zone (arrowed) is difficult to estimate from the available seam contour data and therefore is not included.

in this dataset. Where data is available, strain within a relay zone is best detected by a composite horizon separation diagram (see below).

Throw gradients

High throw gradients within an overlap zone are characteristic of displacement transfer across the zone (Muraoka & Kamata 1983, Walsh & Watterson 1990, Peacock & Sanderson 1991, Childs *et al.*, 1995). These high throw gradients are accommodated by shear strain of the relay zone in the plane parallel to the fault surfaces (fault-parallel shear strain). This shear strain effects the transfer of displacement across the relay zone. A 'high' displacement gradient is defined relative to gradient values typical of isolated faults of similar size (Fig. 4). Except for two measurements of 0.029 and 0.017, the highest throw gradient measured on an isolated fault in this study is 0.015, which is approximately equal to the mean of the relay zone throw gradient values. The upper limit of horizontal throw gradients for isolated coalfield faults has previously been determined as 0.02 (Walsh & Watterson 1989). Gradients >0.015 are therefore taken as indicative of likely displacement transfer between coalfield faults in this size range (maximum displacement ca. 2 m). Ranges of throw gradients are similar for both unlinked and linked overlapping fault segments (Fig. 4).

Although throw gradients >0.015 give a positive indication of displacement transfer between faults, it does not follow that gradients <0.015 are diagnostic of no displacement transfer. A throw gradient is directly proportional to the shear strain in the fault-parallel plane which accommodates it. Calculated values of both throw gradient and shear strain are averages for the region

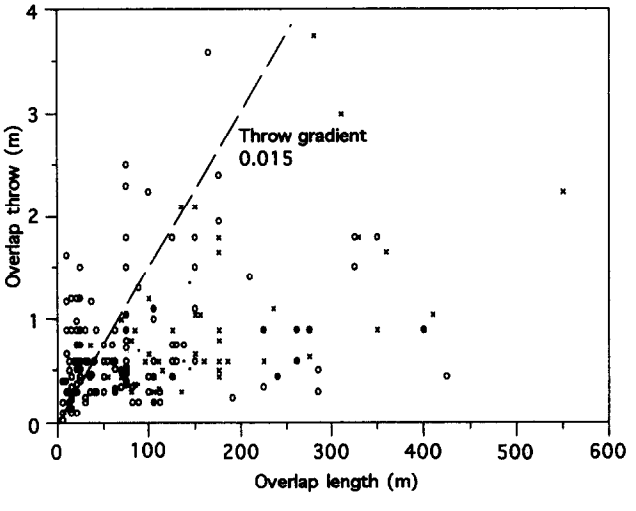

Fig. 4. Overlap throw vs overlap length for 148 individual traces from 114 synthetic overlap zones recorded in British coalfields. Unlinked overlapping fault segments (open circles) and linked overlap segments (filled circles) are distinguished. Also shown are data for 55 isolated coalfield faults (crosses), for which the maximum throw (ordinate) is plotted against half the fault trace length (abscissa). The locus of throw gradients of 0.015 is shown and is the effective upper limit of throw gradient for isolated coalfield faults.

over which they are measured and smaller-scale variations are obscured. Given the wide variation in measured throw gradients, at least partly due to data limitation, throw profile asymmetry and changes in throw gradient are believed to provide a more reliable indication of displacement transfer.

Horizon separation geometries—open-cast data

Geometrical relationships between overlapping fault traces are best examined using composite horizon separation diagrams in conjunction with throw profiles. Composite horizon separation diagrams are constructed by horizontal projection of horizon cutoff lines onto a vertical plane parallel to the fault strike. If regional bedding was horizontal prior to faulting, the vertical interval between the hangingwall cutoff of the footwall fault and the footwall cutoff of the hangingwall fault is a measure of the throw component accommodated by ductile strain of the volume between the overlapping fault traces (Fig. 5b). If there is a component of regional dip in the fault-normal plane, the vertical interval between the two cutoffs will either increase or decrease, depending on the dip direction. Where the apparent dip of regional bedding in the fault-normal plane is in the same direction as the fault dip, the interval between the two cutoffs increases (Fig. 5c). Apparent dip, which is opposed to fault dip, decreases the interval between the cutoffs, which may overlap (Fig. 5d). If fault strike is parallel to the regional dip direction, the apparent dip in the fault-normal plane is zero, with no effect on the vertical interval between cutoffs. The effect of regional dip on the vertical interval between the two cutoffs is given by:

$$\text{change in vertical interval} = s \times \tan \alpha, \quad (1)$$

where s = overlap separation measured normal to the fault surfaces and α = apparent dip of regional bedding in the vertical fault-normal plane. The change in vertical interval is positive if the apparent dip is in the same direction as the fault dip and negative if opposed to the fault dip. Peacock & Sanderson (1994) discussed the effect of regional bed dip on structural contours within relay zones.

The apparent dip of bedding in the fault-normal plane will change if there is a component of shear strain in this plane; such shear strain contributes a component of ductile throw within the relay zone. A component of shear in the fault-normal plane is necessary to accommodate any fault interaction or monocline development which occurs before the fault tips overlap, i.e. during the underlap stage, but may also accompany continued growth and interaction of the overlapping faults. Shear strain in the fault-normal plane increases the vertical separation of the hangingwall cutoff of the footwall fault and the footwall cutoff of the hangingwall fault. The shear strain (γ) is given by:

$$\gamma = \tan \alpha' - \tan \alpha \quad \text{(Escher } et\ al.\text{, 1975)}, \quad (2)$$

where α = apparent dip of regional bedding in the fault-normal plane, α' = observed apparent dip of bedding in the fault-normal plane within the relay zone, and α and α' are positive for apparent dips towards the hangingwall and negative for apparent dips towards the footwall. The component of throw accommodated by ductile deformation is equal to $\gamma \times s$ and provides additional vertical separation of cutoffs.

The characterization of relay zones using composite horizon separation diagrams is illustrated below by two examples.

Daisy Hill open-cast site relay zone, Northumberland. Figure 6(a) shows a relay zone which was mapped from grids (ca. 50 × 50 m) of exploration borehole data from an open-cast coal site. Throw profiles (Fig. 6b) for the two relay bounding fault segments show high (0.06) throw gradients within the relay zone and rapid increases in gradients from the points of overlap into the relay zone. The aggregate fault throw profile shows two minima, coincident with the tips of the two traces, due to ramp rotation extending beyond the overlap area. The combined horizon separation diagram (Fig. 6c) shows that the footwall and hangingwall cutoffs of the composite fault define smooth curves which are locally straight and parallel to the apparent regional dip of bedding. The cutoffs defining the relay ramp are parallel to one another and at a high angle to the apparent regional dip. Within the relay zone, the vertical separation of horizon cutoffs is 3 m.

The contribution of ductile shear strain to the aggregate throw on the structure is calculated as follows. Estimates of the regional bed dip vary from between 0.4° and 2° to 070°, but from the mean plunge of the fault cutoffs (Fig. 6c) is taken to be 0.4°–070°, giving an apparent dip of 0° in the fault-normal plane. Regional dip therefore makes no contribution to the 3 m cutoff vertical separation which is accounted for by a shear strain of 0.05 in the fault-normal plane. When the component of throw due to fault-normal shear strain is added to the aggregated fault throws, a more regular profile results (Fig. 6b), with a gradual decrease in throw from east (Fault A) to west (Fault B). Within the relay zone, the seam dip steepens to 5° (apparent dip in the fault parallel plane of ca. 4°) from a regional dip of 0.4° and the strike is rotated clockwise from the regional strike of NNW; shear strain in the relay zone in the vertical fault-parallel plane is ca. 0.06, which is equivalent to ca. 0.07 for a fault dip of 60°.

West Chevington open-cast site relay zone, Northumberland. The map shown in Fig. 7(a) was constructed from extraction plans, which provide a more accurate definition of the structure of the relay zone than in the previous example. Maps of this relay zone on three other seams have recently been published by Peacock & Sanderson (1994). Their study provides a good general description of the relay zone and makes reference to the significant component of ductile strain within the relay zone. Here we describe the displacement variations on component faults and quantify strain variation within

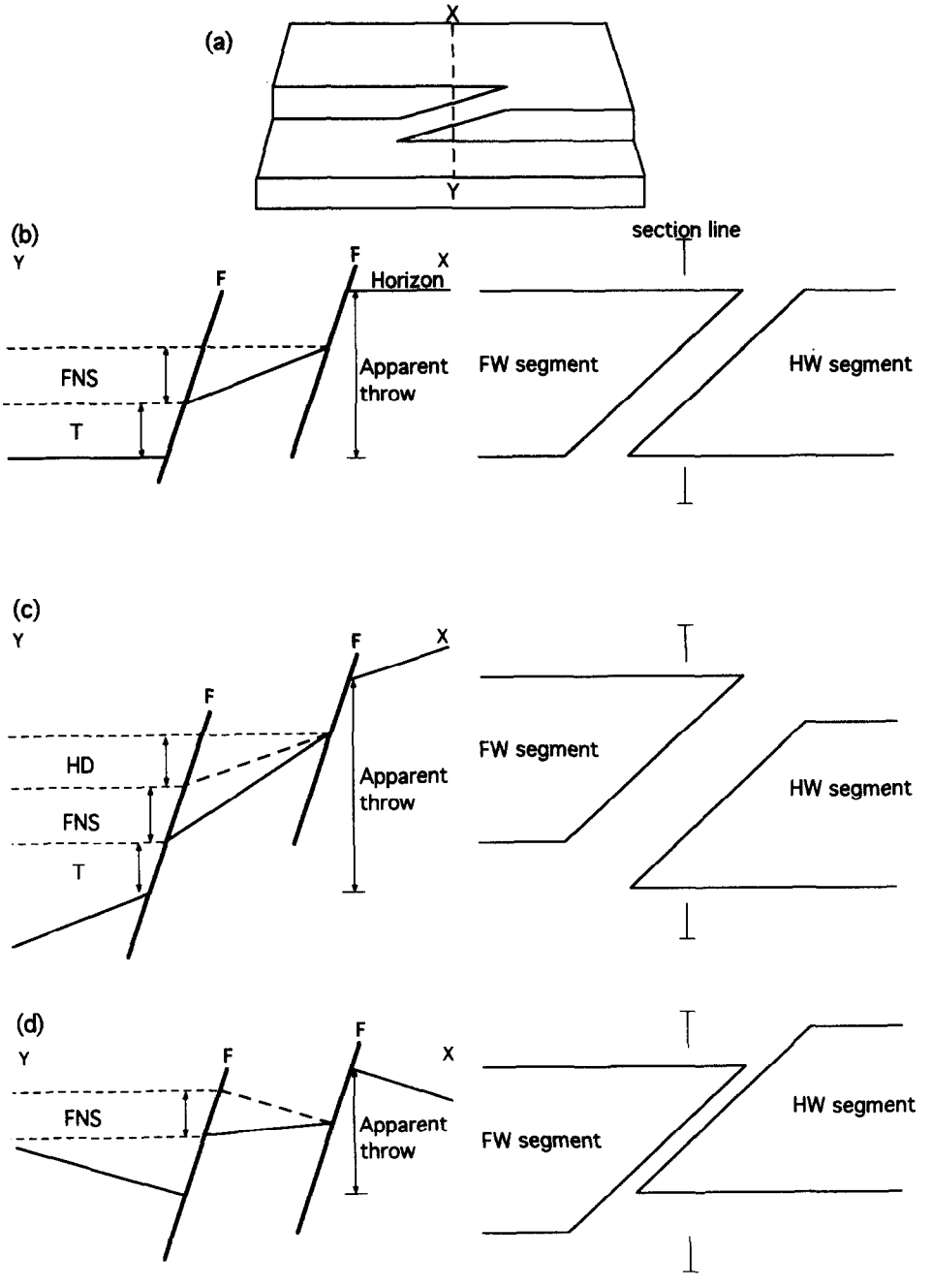

Fig. 5. Schematic cross-sections (normal to fault-strike) and composite separation diagrams of a relay zone showing the effect of variation in apparent regional dip in the strike-normal plane on the apparent throw across a relay zone. The apparent throw across the relay zone is the difference in elevation from the uppermost footwall cutoff to the lowermost hangingwall cutoff. The apparent throw may be comprised of shear in the fault-normal plane (FNS), fault throw (T) and a horizon dip component (HD). The separation diagrams are drawn assuming the apparent horizon dips shown in the cross-sections are true dips and the fault-normal shear strain and fault throw are the same in each case. (a) Schematic diagram illustrating horizon geometry at a relay zone. The line of cross-section is marked *X*–*Y*; three geometries are illustrated: (b) zero apparent dip; (c) apparent dip and fault dip in the same direction; and (d) apparent dip opposed to fault dip.

the relay zone. The footwall fault (A) has a synthetic splay (C). The aggregate throw profile of Faults A and C (Fig. 7b) shows an abrupt increase in throw gradient, from 0.02 outside the relay zone to 0.11 within the relay zone, to complement the high gradient of 0.08 on Fault B. The aggregate throw of Faults A, B and C decreases from east to west (Fig. 7b), with a throw minimum coincident with the relay zone.

The regional bedding varies in strike from 035° in the east to 000°; the average regional dip is 3.5° towards 115° with an apparent dip in the fault normal plane of 1.5° opposed to the fault dip. The mean overlap separation is 80 m and, in the absence of any shear strain within the relay zone, 2.1 m of vertical overlap of the relay zone bounding cutoffs would be expected on an horizon separation diagram. However, the cutoffs do not overlap and there is a vertical separation of ca. 4 m within the relay zone (Fig. 7c). The total change in bed elevation across the relay zone due to fault-normal shear strain is therefore 6.1 m, which is equivalent to a shear strain of

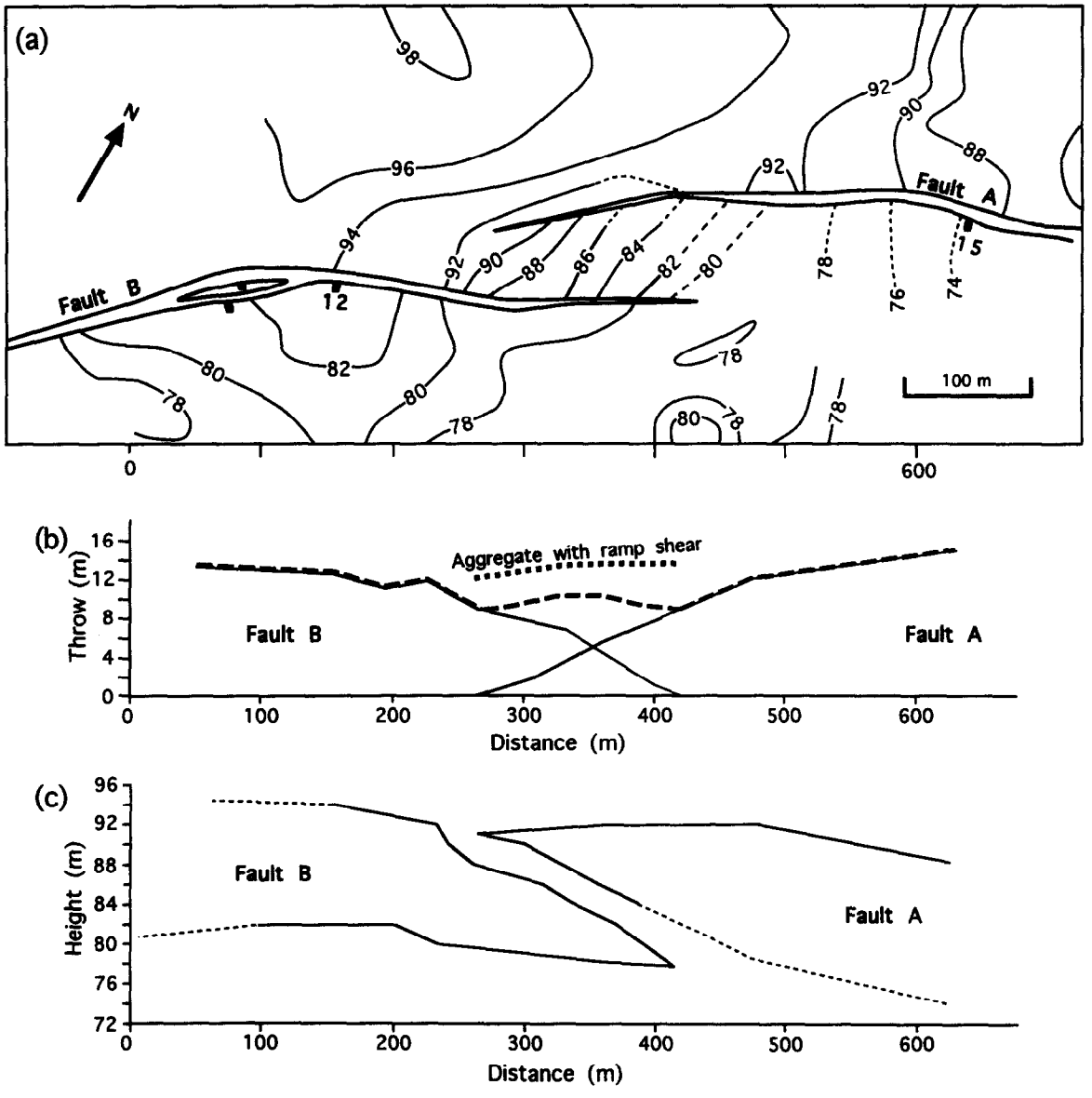

Fig. 6. Relay ramp at Daisyhill open-cast coal site, Northumberland. (a) Map of fault segments A and B on the Main Seam, from the British Coal Exploration Geological Plan, showing recorded fault throw values (m), throw directions (ticks on downthrown sides) and seam elevation contours in m, broken contours are poorly constrained; (b) throw profiles of fault segments A and B (solid line) in the region of the relay zone, aggregate fault throw (broken line) and aggregate throw, including the ductile shear strain component (broken line, labelled); (c) composite horizon separation diagram for fault segments A and B.

0.08. Adding the effects of this shear strain to the aggregate throw profile removes the aggregate throw minimum (Fig. 7b).

Beds in the ramp steepen to as much as 8° from the regional 3.5° dip and strike changes are generally ca. 45° anticlockwise of regional bedding. The apparent dip of bedding in the ramp in the fault-parallel plane results from two factors. The first is the apparent dip of regional bedding on the fault-parallel plane, and the second is the shear strain within this plane which accommodates the throw gradients within the relay zone. In this case, the regional bedding apparent dip is 3.4°, in the same direction as the tilt due to the fault-parallel shear strain, so the two components are additive. The fault-parallel shear strain of the ramp is at its highest value of 0.087 (for a fault dip of 70°) towards the centre of the relay zone, where most of the displacement transfer occurs.

Bed orientation within the relay ramp is therefore a function of three variables, namely (i) relative orientation of faults and regional bedding; (ii) shear strain in the fault-normal plane; and (iii) shear strain in the fault-parallel plane. The deviation of cutoff lines within the overlap zone from their overall trend (angle β in Fig. 7c) is a measure of the fault-parallel shear strain ($\gamma = \tan \beta$) accommodating displacement variation.

Relay zone shapes—statistics

Two outstanding questions concern (i) the attributes of relay zones which are associated with high throw gradients, i.e. a high degree of displacement transfer; and (ii) changes of throw gradient during relay zone growth. Relay zone attribute data collated to investigate

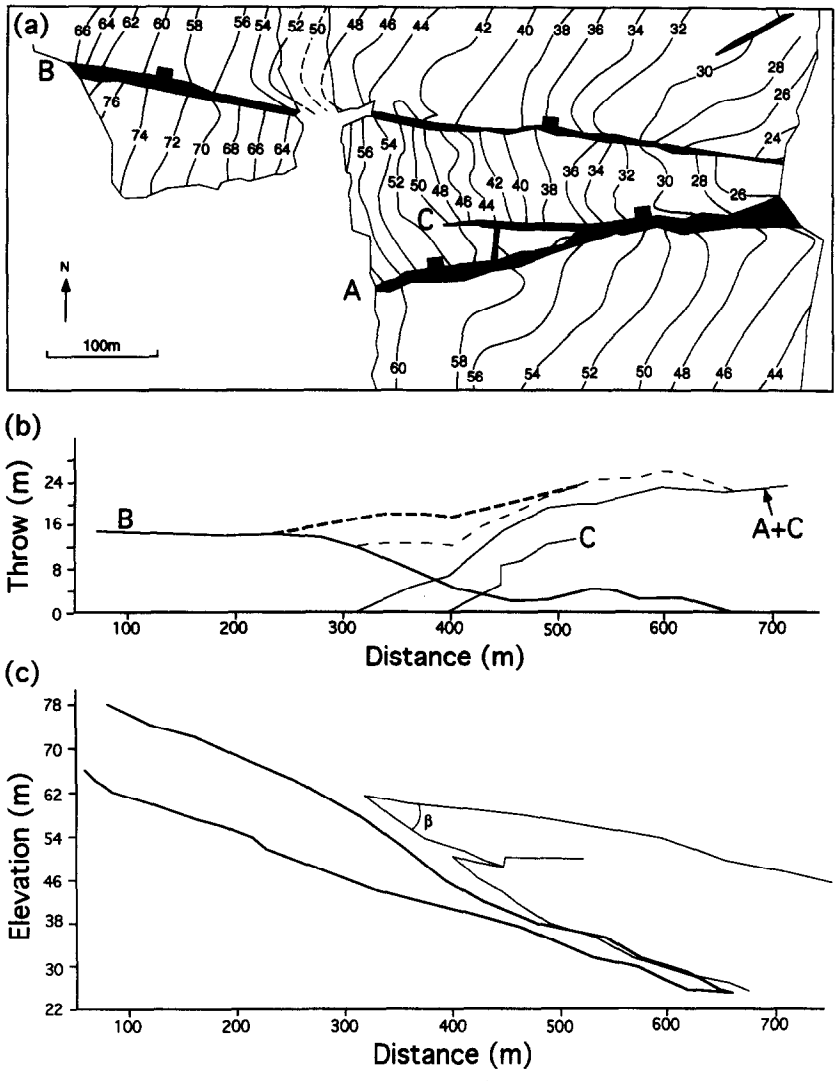

Fig. 7. Relay ramp at West Chevington East Extension open-cast site, Northumberland. (a) Seam map with fault segments A and B and splay C (black fill) from the extraction plan for the Main Seam. Seam elevation contours are in m. (b) Throw profiles for segment B (heavy solid line), splay C (thin solid line) and the aggregate of segment A and splay C (also thin solid line). The aggregate fault throw (thin broken line) and aggregate throw including the ramp shear strain (heavy broken line) are shown; (c) composite horizon separation diagram with cutoffs of fault segment A and splay C (light solid line) and segment B (heavy solid line).

these problems included overlap zone dimensions, throws and throw gradients for 114 overlap zones.

A broad positive correlation between overlap length and overlap separation, and a maximum observed aspect ratio (length/separation) of 20 (Fig. 8) are simply functions of the criteria used to identify overlap zones. No unequivocal, simple relationship between overlap zone attributes has been identified by analysis of the quantitative relay zone data. Apart from a weak indication that, for a given length and maximum throw (on bounding faults), smaller separations are associated with higher throw gradients, the data do not demonstrate any clear relationship between overlap zone attributes, such as throw gradient, separation and overlap length. Of the several possible reasons for the absence of simple relationships, the limitations of two-dimensional attributes are likely to be the most important. Since two-dimensional data provide no information on the three-dimensional geometry of relay zones, such as the orientation of a tip-line with respect to the mapped surface, measurements made from two-dimensional data are inevitably ambiguous.

THREE-DIMENSIONAL CHARACTERISTICS

Confident interpretation of the three-dimensional form of a relay zone is possible only with a good match between the size of a relay zone and the number and spacing of seams on which the structure is recorded. Few structures in the analysed dataset meet this requirement and the best example, at Glapwell Colliery, is described below, together with a reconstruction of its successive growth stages. A less complete example from Markham No. 2 Colliery is also described.

Glapwell relay zone

Geometry. This structure is recorded on five seams over a vertical interval of 270 m. Discontinuous overlapping fault traces occur on three seams and continuous

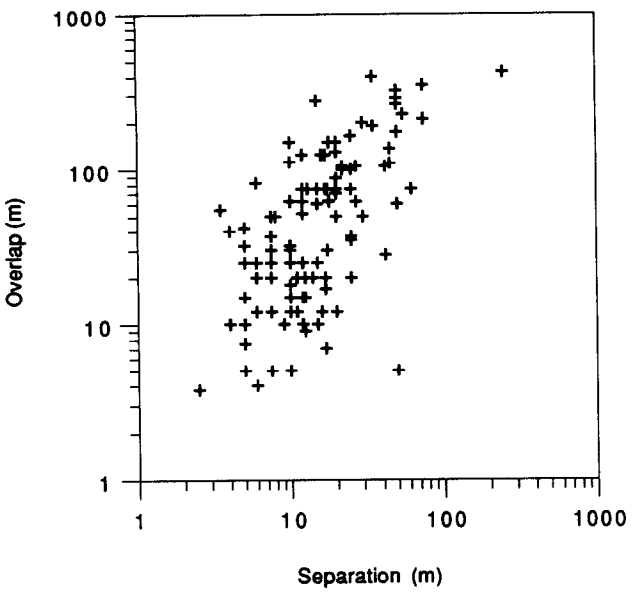

Fig. 8. Overlap length vs separation for 114 coalfield overlap zones.

fault traces occur on the topmost and lowermost seams (Fig. 9). The relay zone therefore represents a hole, or tunnel, through the fault surface, with its axis sub-parallel to the fault surface. The tunnel walls are two salients, or lobes, each continuous with the main fault surface and referred to as the footwall and hangingwall lobes. On the topmost seam, the continuous fault trace is convex towards the footwall side of the fault and is interpreted to immediately overlie the upward closure of the overlap zone. On the lowermost seam, the continuous fault trace is almost straight, with a short footwall splay, and is interpreted to immediately underlie the downward closure of the structure. Between the upward and downward closures the footwall lobe, when viewed from the hanging-wall side, is continuous with the main fault surface on the right and terminates to the left mostly along a tip-line (Fig. 10). Conversely, the hangingwall lobe is continuous with the main fault surface on the left and terminates to the right at a tip-line.

Divergence of the lobes at the lower closure of the structure is accommodated primarily by a change in strike of the footwall lobe and a steepening of dip of the hangingwall lobe. Changes of dip of parts of the fault surface are essential elements of the structure and are shown by structural contours on the fault surface shown in Fig. 10, together with three cross-sections. Dip changes are not restricted to the lobes, but also occur on the parent fault surface beyond the lobes; the dip changes of the parent fault surface are crucial to interpreting the growth stages of the overlap structure. The dips shown are those derived from the locations of traces on successive seams, and necessarily incorporate the assumption that dip changes in cross-section occur only at coal seams; true cross-sectional profiles will be smoother than those shown in Fig. 10(b).

In addition to their transitional junctions with the main fault surface, the lobes are bounded mostly by tip-lines but probably also by relatively short branch-lines, as indicated in the perspective view (Fig. 11) and in the strike-projection of the main fault surface, i.e. projection onto a vertical plane parallel to the fault strike (Fig. 12). The precise extents of the branch-lines are difficult to determine, but they are certainly restricted to the uppermost and lowermost parts of the relay structure. Junctions of lobes with the main fault surface are not primarily along branch-lines but along transitional junctions, or tilt axes (Hull 1993), with the lobes simply extensions of the main fault surface.

The relay zone is thus a closed structure lying within the parent fault surface, with a maximum separation of lobes of ca. 25 m, a lateral lobe overlap of ca. 100 m and a longest dimension of ca. 200 m, i.e. the overall form is approximately prismatic with principal dimensions in the ratio ca. 8:4:1. The major axis of the structure lies obliquely within the parent fault surface pitching ca. 75° to the east. As the maximum throw on the main fault surface lies below and to the right of the relay zone (Fig. 12), the alignment of the relay zone on the main fault surface is approximately normal to the throw contours and to the advancing tip-line. If the fault surface is elliptical (Rippon 1985, Walsh & Watterson 1989), this alignment is eccentrically radial with respect to some point on the major axis of the ellipse lying between the centre and the focus.

Displacement pattern. Aggregate throw contours on the fault surface define approximately concentric curves about the maximum recorded throw (Fig. 12). There is no indication that the two lobes were previously isolated fault segments with their own distinct throw maxima and it appears that the fault, with its two overlapping lobes, evolved as a single coherent kinematic unit. The re-entrant in the 2 m contour may be an artefact arising from the chosen contour value, but could be due to ductile strain within the relay zone. Throw profiles (Fig. 2c) clearly show transfer of throw between the two lobes.

Growth sequence. A series of likely growth stages of the relay structure is shown in Fig. 13: all views are from the hanging-wall side. (a) Before the structure is initiated, the tip-line of the main fault surface is locally straight and propagates radially, leftwards and upwards, with respect to a point on the horizontal principal axis; (b) tip-line propagation is retarded at one point because of an obstacle in the form of a material anisotropy. The tip-line continues to propagate on either side of the obstacle, creating an embayment in the tip-line; (c) the tip-lines of the lobes propagate towards one another in the lee of the material anisotropy; (d) the lobes on either side of the embayment are not co-planar and the tip-lines on opposite sides of the embayment do not meet but propagate past one another and begin to overlap. The western lobe (left) dips more steeply than the main fault surface and becomes the hangingwall lobe; (e) continued lateral growth causes the lower tip-line of the hangingwall lobe to intersect the main fault surface forming a branch-line at the approximate position of the

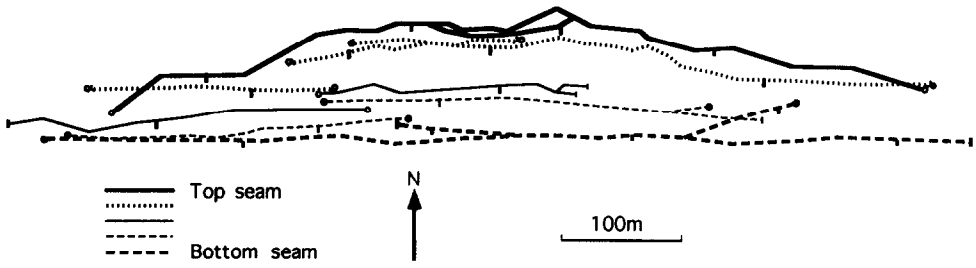

Fig. 9. Trace geometries on five seams of a fault containing a relay zone at Glapwell Colliery, Derbyshire, projected vertically onto a common horizontal surface. Fault traces recorded from each seam are shown with different line ornaments. Fault trace tip-points (open circles), ends of workings (bars) and throw directions (ticks) are shown. The fault has a continuous trace only on the top and bottom seams. The seam dips are 2.8° to the east.

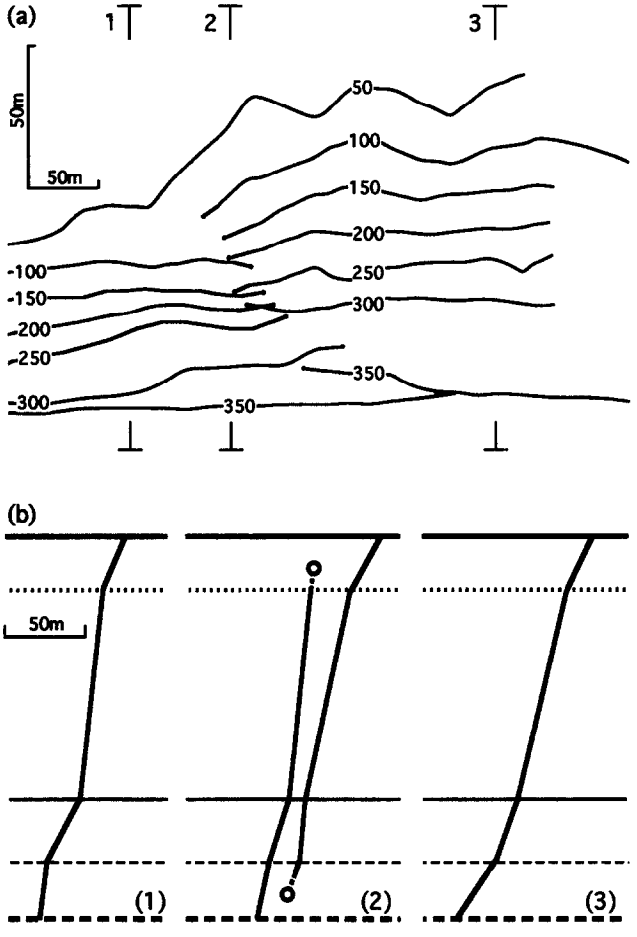

Fig. 10. (a) Plan view of structural contours on the fault surface, derived from the fault traces shown in Fig. 9, in the region of the relay zone. Contour spacing is 50 m and depths are below an arbitrary datum. Locations of cross-sections in (b) are indicated; (b) cross-sections through the region shown in (a) are viewed from the right (east). Seam ornaments are the same as in Fig. 9.

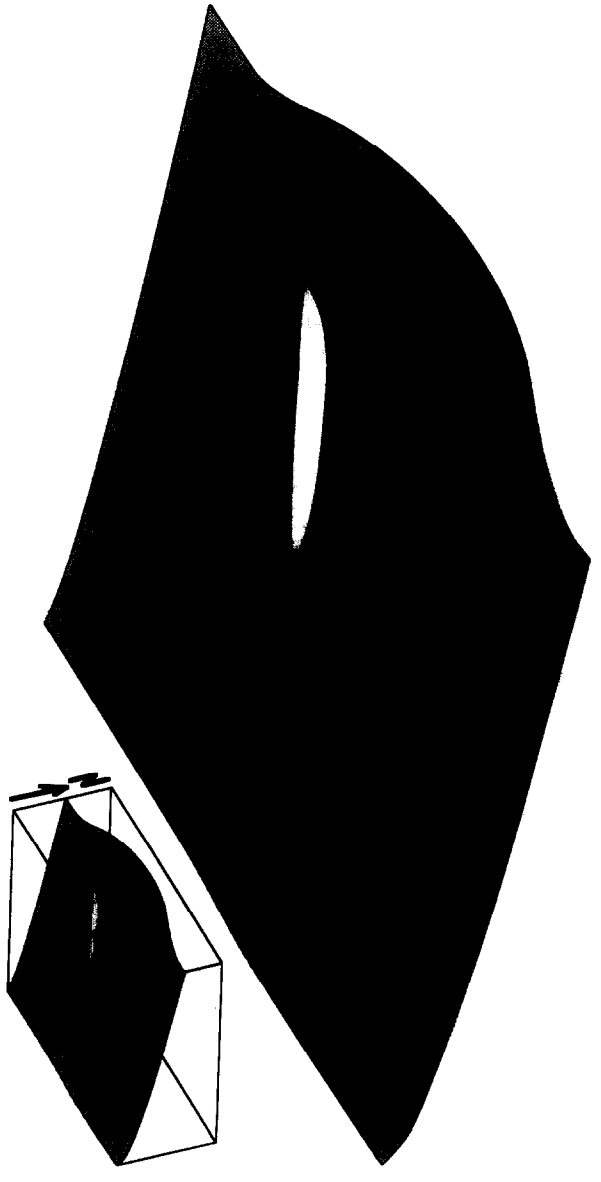

Fig. 11. Perspective diagram of the Glapwell Colliery relay zone, shown in Figs. 9 and 10, viewed from the southeast. The fault surface is shaded. Form lines on the fault surface (light solid lines), fault tip-lines (medium solid lines and light broken lines) and branch-lines (heavy solid lines) are shown.

initial embayment; (f) the footwall lobe grows to merge with the hangingwall lobe both proximally, at the point of original embayment, and distally, close to the overall fault tip-line. Footwall lobe propagation obliquely upwards and to the left is accompanied by a progressive steepening with upward change of strike, resulting in the curvature of the lobe towards the hangingwall. Once the two lobes have linked, the overlap zone is closed and there is again a single tip-line to the main fault surface; (g) the fault tip-line continues to propagate upwards but is curved in the lee of the relay structure (Fig. 10a). As fault propagation continues, the fault tip-line becomes progressively straighter. The present-day structure is at this stage of development; (h) further accumulation of displacement on one or both of the overlapping lobes would have caused further tip-line propagation and the

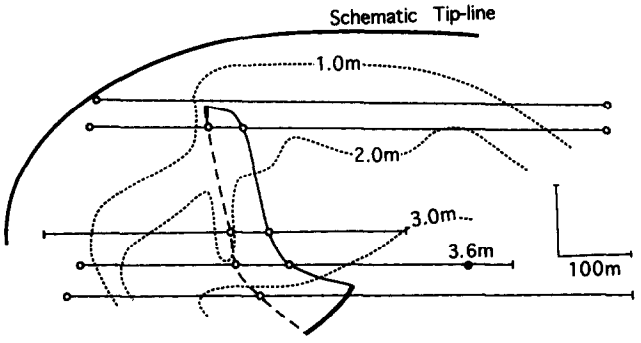

Fig. 12. Strike projection of that part of the Glapwell Colliery fault surface containing the relay zone, viewed from the hangingwall. The five fault/seam intersections are shown as sub-horizontal lines. The relay zone is bounded by the hangingwall lobe tip-line (medium solid line), the footwall lobe tip-line (broken line) and two short branch-lines (heavy solid lines). Aggregate throw contours on the fault surface are shown as dashed lines (contours are based on 49 throw values). The point of maximum throw on the fault surface is interpreted as lying below and to the right of the part of the fault surface illustrated. Based on the location of the maximum throw, the overall tip-line, which is not well defined by the data, is interpreted as having propagated upwards and to the left.

advancing tip-lines would have been gradually replaced by static branch-lines as they intersected the main fault surface.

Had the replacement of tip-lines by branch-lines happened at the same time on both lobes, the rock volume within the relay zone would have become totally enclosed by the lobes to form a horse. Had one lobe become completely bounded by a branch-line before the other, then it would have remained an active part of the main fault surface and the other lobe would have become a 'dead' splay (Childs *et al.*, 1995) (Fig. 13h). In both cases the relay zone could be said to have been breached, although breaching of a relay zone at one level does not mean that the whole structure is breached and inactive (Peacock & Sanderson 1994).

With this growth model, a relay zone is initiated by simple retardation of propagation at one point on a locally straight tip-line, which we assume to be a relatively common occurrence. The formation of segmented faults by this process is analogous to cross-slip of screw dislocations when they meet an obstacle as described by Jackson (1987). The proposed model of formation of the Glapwell relay zone indicates that, for faults, an edge-type tip-line may also become segmented when it meets an obstacle.

Tip-line geometries similar to those described for the Glapwell example have been observed in the successive positions of ultrasonically modulated Mode I crack tips in glass (Kerkhof 1973, Green *et al.*, 1977, Bahat 1991). For a crack tip approaching a hard inclusion, the tip-line becomes bowed around the obstacle (Figs. 14 and 13 a & b) and the tip propagation rate is locally reduced. Where a tip-line approaches a relatively soft inclusion (e.g. a pore space), the tip-line bows outwards to meet the inclusion (Peter 1968, Green *et al.*, 1977). Once the crack has propagated through the inclusion, the crack surface may be either planar with a straight tip, or segmented. Green *et al.* (1977) observed that, in the latter case, 'sometime after the primary crack front has passed on' a secondary fracture occurs which links the two primary cracks. 'Tails' formed in the lee of an inclusion by this mechanism occur in both porous and particulate composites. This manner of crack propagation through an inclusion exhibits the same geometry as the model proposed for the formation of the Glapwell structure.

A bend in a crack surface can be created with a straight propagating tip-line, but only if the bend axis is parallel to the tip-line (Hull 1993); a twist in the crack surface cannot form if the tip-line is straight (Hull 1993). However, once an embayment in the tip-line is formed, the tip-lines on either side of the embayment can each propagate out-of-plane and independently of one another, with each bending along an axis which is parallel to the local rather than the overall tip-line; such bends are effectively twists with respect to the main crack surface. Although such rules are strictly applicable only to perfectly brittle materials, the general concepts are relevant to rocks. In the Glapwell example, the bend axis of the hangingwall lobe is subhorizontal (Fig. 13d), resulting mainly in a change of dip. The bend axis of the footwall lobe is steep, resulting mainly in a change of strike.

The growth direction of the Glapwell overlap zone is inferred to have been parallel to the long axis of the structure both by analogy with the geometry of propagating cracks and because of its position and orientation with respect to the point of maximum displacement, and presumed point of origin, of the main fault. The mechanism proposed not only permits a relay zone to develop but indicates that a discontinuity and eventually a relay zone is the almost certain consequence of a tip-line irregularity.

Markham No. 2 relay zone

Geometry. Data for the lower part of a relay zone (Fig. 15) are shown in plans of five worked seams from Markham No. 2 Colliery, North Derbyshire, which occur over a vertical interval of 200 m. The three upper seams have overlapping fault traces with separations which increase upwards from 25 to 37 m and the maximum overlap length of ca. 200 m occurs on the topmost seam. On the seam immediately underlying these three the fault trace has a bend with an amplitude of ca. 30 m and on the lowermost seam the trace is gently concave towards the hangingwall. The data volume contains only the lower closure of the relay zone which occurs either as a branch-point or as a short branch-line not exceeding 50 m in length. The footwall lobe dips 76° both within and without the relay zone, whereas the hangingwall lobe dip increases from 83° without the relay zone to subvertical within it and is even reversed in places. The lateral tip-lines of the two lobes converge downwards towards the bottom closure of the relay zone; the hangingwall lobe tip-line pitches 33° to the west, and the footwall lobe tip-line pitches 70° to the east. The line bisecting the angle between the downward converging tip-lines, taken as the long axis of the structure, pitches

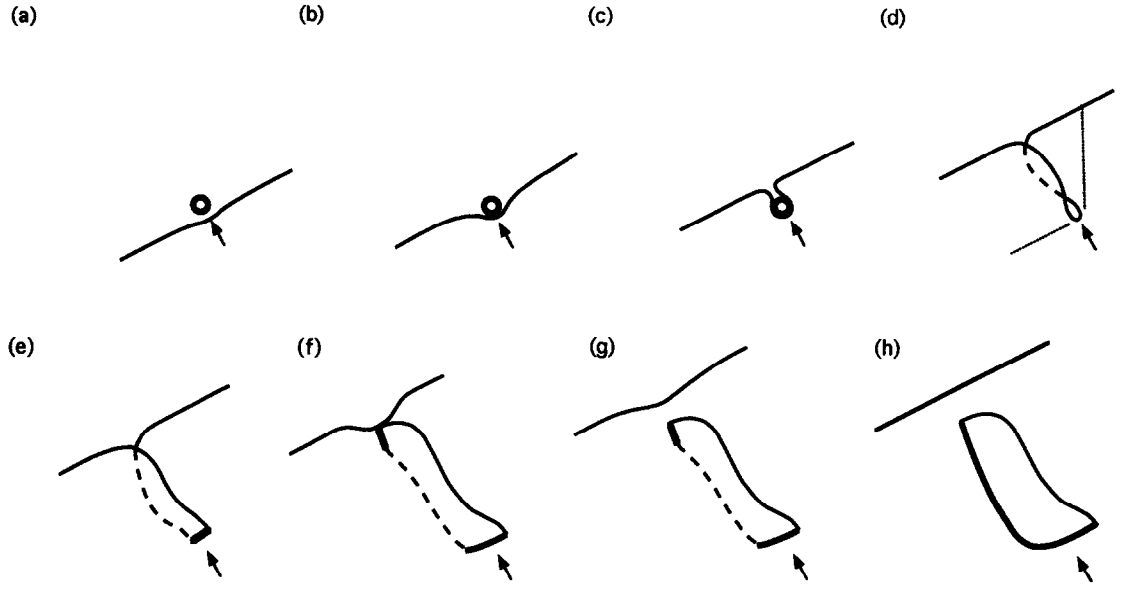

Fig. 13. Schematic diagrams illustrating the interpreted stages of growth, (a)–(h), of the Glapwell Colliery relay zone. The open circle in (a)–(c) represents a lithological heterogeneity which locally retards propagation of the tip-line. Fault tip-lines are shown with a solid line but where the tip-line of the footwall lobe is obscured by the hangingwall lobe, the line is dashed. Branch-lines are shown as heavy solid lines and the initial point of retardation of the overall tip-line is indicated by an arrow pointing in the direction of propagation of the overall tip-line. Dotted lines (d) indicate axes of bending on the fault surface.

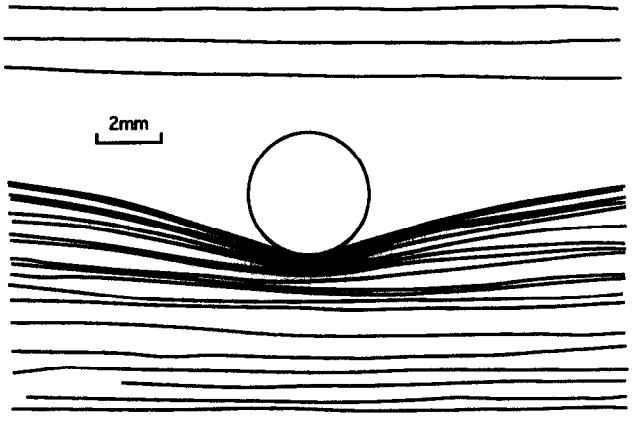

Fig. 14. Line drawing of an electron photomicrograph of an ultrasonically modulated Mode I crack in glass containing a crystalline inclusion, from Kerkhof (1973). The lines indicate successive positions of the upwardly propagating crack front, or tip-line.

ca. 70° to the left when viewed from the hangingwall side. The asymmetry of the throw contours on each lobe is an indication of displacement transfer between the lobes. Each lobe shows a distinct throw maximum (Figs. 16a & b) and there is a marked throw minimum on the main fault surface immediately below the closure (Fig. 16c). The maximum throw on the main fault lies beyond the data area shown, above and to the right of the overlap structure.

Growth sequence. The throw distribution on the main fault surface is consistent with the relay zone long axis being eccentrically radial and having formed on a tip-line propagating downwards and to the left. The single closure seen is, on this basis, that which formed when the two lobes rejoined the main fault, restoring a single tip-line configuration. The throw minimum below this closure is believed to be complemented by high ductile strain associated with the closure of the relay zone. With further fault growth, this element of ductile displacement would be a decreasing proportion of the total displacement and the contoured throw minimum would gradually disappear.

DISCUSSION

Segmentation processes and relay zone formation

Relay zones and segmented fault systems are formed either by overlap of independently nucleated faults or by the formation of en échelon or en bayonet fault segments which are kinematically related throughout their existence and often link out-of-plane into a single fault surface (Larsen 1988, Childs *et al.* 1995). Incidental overlap zones will be more common in areas of high fault density where fault interaction is more likely to occur. The formation of segmented faults by out-of-plane bifurcation of a single fault surface can occur in a variety of ways. Segmentation resulting from movement on faults which are slightly oblique or, in the case of curved faults, locally oblique to the regional stretching direction has been described by Childs *et al.* (1995). In other cases, e.g. Timor Sea (Woods 1992), oblique reactivation of a single basement fault, with the later extension at ca. 75° to the fault strike, has lead to the formation of en échelon faults within an overlying cover sequence which may either die out at depth or link into the basement fault (Larsen 1988, Woods 1992). Segmented faults associated with forced folding and monocline development are formed within a cover sequence by reactivation of a basement fault (Withjack *et al.* 1990) but, in these examples, the segmented faults may not have been

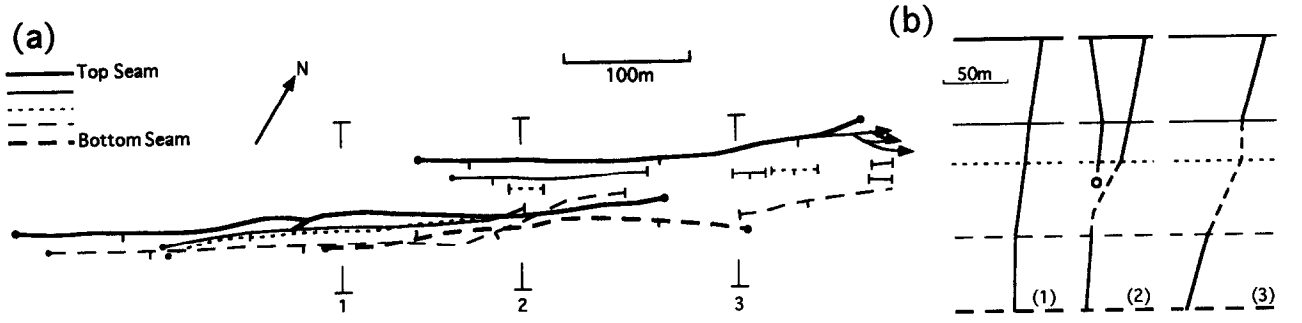

Fig. 15. (a) Fault trace geometries, on five seams, of part of a relay zone at Markham No. 2 Colliery, North Derbyshire, projected vertically onto a common horizontal surface. The fault has a continuous trace on the bottom two seams. Fault trace tip-points (open circles), ends of data (bars), truncated data (arrow heads) and throw directions (ticks) are shown. Seam dip is 4.5° to the northeast. Locations of the cross-sections shown in (b) are indicated; (b) cross-sections through the fault, viewed from the right (east).

rooted in the basement fault, at least in the initial stages of cover faulting. Examples of fault segmentation due to uneven propagation of a fault tip-line attributed to variable fracture toughnesses of the host rock have been described above. We believe that, for faults which propagate through mechanically heterogeneous media, the formation of segmented faults by this mechanism is a common occurrence.

Displacement gradients

Why, and how, do the tip regions of overlapping faults bounding a relay zone sustain higher displacement gradients than the tip regions of single, isolated faults? Displacement gradients are unlikely to be limited by material restrictions on permanent strain values because, given time, most rocks can sustain unlimited Mode III permanent strains. A limit may exist to the permanent Mode II strain which can be imposed on some rock types because of the volume changes required. A more likely control on displacement gradient is the local elastic strain which accommodates each slip event and which is transformed to a permanent strain before the succeeding slip event re-imposes the elastic strain. This local elastic strain is not to be confused with the regional elastic strain which drives the faulting, and which is partly *relieved* by a fault-slip event. The local elastic strain imposed by a fault slip event represents the heterogeneous strain required to accommodate slip variation over a finite surface bounded by a tip-line.

The maximum slip (U) on an isolated fault in a single slip event is linearly related to the linear dimension (L) of the slip surface (Scholz & Cowie 1990). The ratio of the two values is a function of the material properties of the rock and is proportional to the elastic shear strain ($\gamma = 2U/L$). The elastic shear strain imposes a shear stress which exerts a force tending to propagate the tip-line. The propagating force is a function of both the elastic shear strain and the shear modulus and is resisted by a force which is a function of the fracture toughness. For a given maximum slip value, the fault will propagate, with the elastic shear strain reducing as L increases, until the propagating force reduces to a level at which it is balanced by the resisting force.

At an overlapping fault tip-line, the propagating force generated by a given elastic shear strain is less than in the general case because, within the relay zone, only a relatively thin sliver of rock is elastically strained, as opposed to the larger strained volume associated with the corresponding part of an isolated fault. Overlapping fault tip regions can thus accommodate higher elastic shear strains, and hence higher elastic displacement gradients, than are possible on isolated faults, but only if the overlapping faults are active at the same time. The cumulative shear strains and displacement gradients associated with relay zones are therefore also higher than those typical of isolated fault tip regions. The tip-line propagating force associated with a given elastic shear strain is expected to decrease with increase in overlap length and with decrease in overlap separation. The effective reduction of the propagating forces on the tip-lines of two overlapping faults is therefore the mechanism by which displacement transfer between the two faults is achieved.

CONCLUSIONS

(1) The term relay zone is used where there is evidence for interaction between the two overlapping fault traces. Asymmetry of the throw profiles along the two fault traces bounding a relay zone is an indication of interaction; the asymmetry is due to steepening of throw gradients within the relay zone. Throw profiles on overlapping fault traces are complementary and usually provide an aggregate throw profile which is similar to that of an equivalent continuous single fault trace.

(2) Throw gradients on fault traces bounding relay zones may be steeper than gradients on isolated faults, but in many relay zones the steeper gradients are within the range associated with isolated faults. High throw gradients are possibly associated with low separation values for overlaps of given length and bounding fault maximum throw. The orientations of the fault tip-lines relative to the mapped surface is likely to be crucial to understanding observed two-dimensional relationships

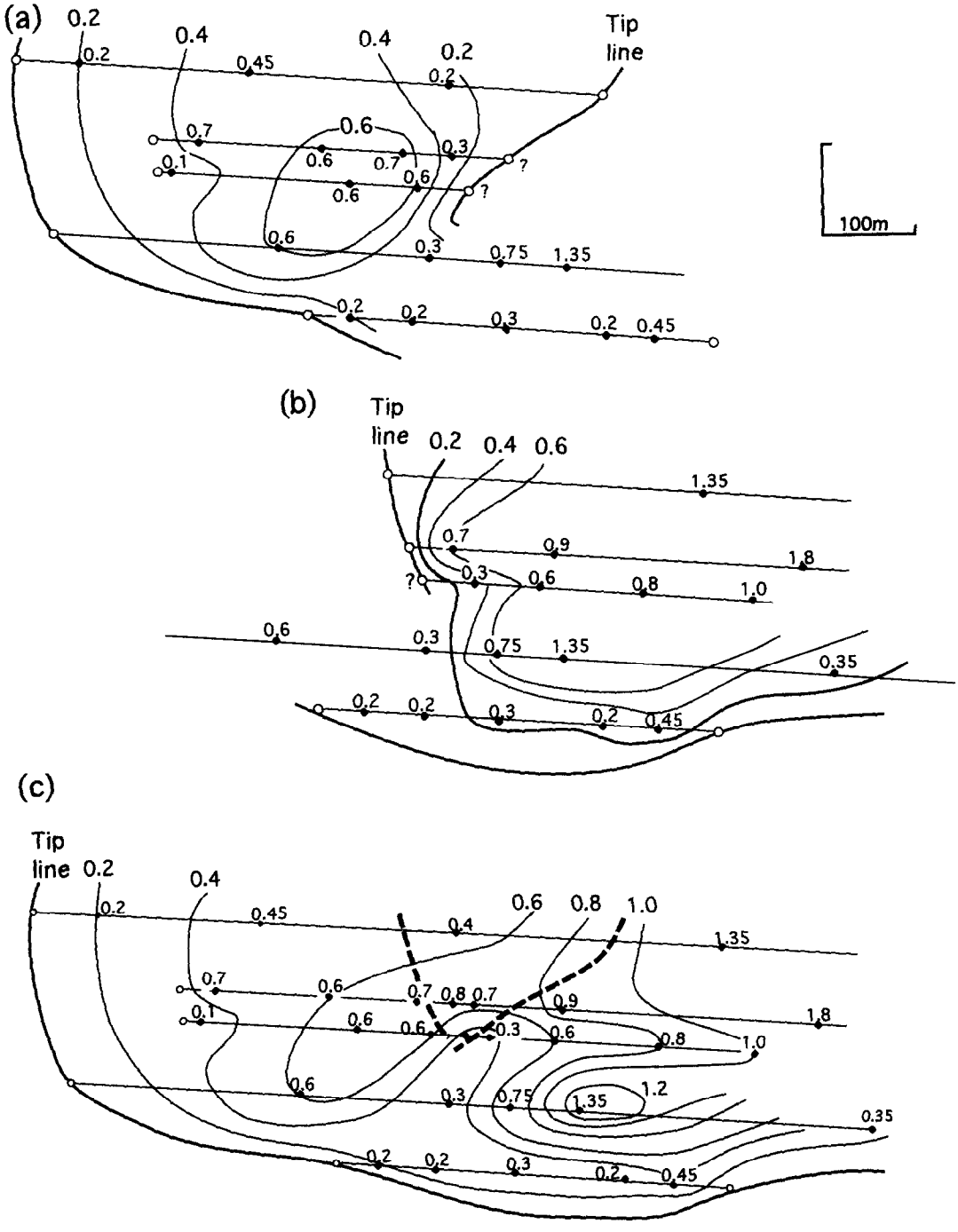

Fig. 16. Strike projections of the Markham No. 2 Colliery fault containing a relay zone of two individual overlapping lobes, viewed from the hangingwall. Only the lower part of the overlap structure is contained within the data volume. Fault/seam intersections are shown as sub-horizontal lines with recorded throw values (m) attached. Recorded tip-points shown as open circles. (a) Hangingwall lobe; (b) footwall lobe. Throw contours are shown at zero throw (tip-line), 0.2 m, 0.4 m and 0.6 m; (c) combined fault surface. Tip-lines of the overlapping fault lobes are shown as heavy broken lines. Aggregate throw contours are shown from zero throw (tip-line) to 1.2 m at 0.2 m intervals.

between relay zone sizes, aspect ratios and throw gradients.

(3) Shear strain of the relay zone occurs in both fault-parallel and fault-normal planes. Shear in the fault-normal plane may extend laterally beyond the limits of the relay zone, giving rise to an apparent low in aggregate throw coinciding with the relay zone.

(4) Where the data permit, important aspects of the geometries of relay zones are most clearly shown by composite horizon separation diagrams. These diagrams show the effects of the relative orientations of the regional horizon dip and the fault dip on the apparent dips within the relay ramp, in both the fault-parallel and fault-normal planes. Shear strains parallel to these planes can also be evaluated but a shear strain in the fault-normal plane is not essential to the formation of a relay zone. The directions and amounts of horizon dips within a relay zone are determined by the size of the relay zone, the regional dip direction relative to that of the faults and the shear strains in both the fault-normal and fault-parallel planes.

(5) Relay zones originate either by the incidental

approach of two independently nucleated fault surfaces, or by the bifurcation of a single fault surface. In each case, continued growth of the fault or faults after formation of the relay zone may lead to breaching.

(6) The formation of a well-constrained, three-dimensional example of a relay zone from an initial single fault surface is attributed to local retardation of a straight tip-line, causing bifurcation of the fault surface. Growth of the relay structure eventually results in distal closure with the overlapping lobes enclosing a hole in the fault surface. Further fault growth occludes the hole either by formation of a link fault or by further propagation of one or both lobes. Although separation distances vary with position on an individual relay structure, the wide size range of observed relay zones suggests that new ones are constantly being formed during growth of a fault system, while others are being breached.

(7) The interaction between two overlapping faults arises from the reduction in tip-line propagating shear stress for a given elastic shear strain accommodating a slip event; this change is due to the presence of only a relatively narrow sliver of rock within the relay zone separating the two fault tip regions.

Acknowledgements—The work was part-funded by Amerada Hess Ltd and by Amoco (U.K.) Exploration Company. We are grateful for access to data provided by the former British Coal Corporation. We thank members of the Liverpool Fault Analysis Group for useful discussions, and Chris Bonson and Isabel Jones for preparation of diagrams. We thank P. H. Larsen, C. K. Morley and D. C. P. Peacock for their helpful reviews.

REFERENCES

Aydin, A. & Schultz, R. A. 1990. Effect of mechanical interaction on the development of strike-slip faults with échelon patterns. *J. Struct. Geol.* **12**, 123–129.

Aydin, A. & Nur, A. 1982. Evolution of pull-apart basins and their scale interdependence. *Tectonics* **1**, 91–105.

Bahat, D. 1991. *Tectonofractography*. Springer-Verlag, Berlin.

Cartwright, J. A., Trudgill, B. D. & Mansfield C. S. 1995. Fault growth by segment linkage: an explanation for scatter in maximum displacement and trace length data from the Canyonlands Grabens of SE Utah. *J. Struct. Geol.* (in press).

Childs, C., Watterson, J. & Walsh, J. J. 1995. Fault overlap zones within developing normal fault systems. *J. geol. Soc. Lond.* **152**, 535–549.

Cowie, P. A. & Scholz, C. H. 1992a. Physical explanation for displacement–length relationship for faults using a post-yield fracture mechanics model. *J. Struct. Geol.* **14**, 1133–1148.

Cowie, P. A. & Scholz, C. H. 1992b. Growth of faults by accumulation of seismic slip. *J. geophys. Res.* **97**, 11085–11095.

Cruikshank, K. M., Zhao, G. & Johnson, A. M. 1991. Analysis of minor fractures associated with joints and faulted joints. *J. Struct. Geol.* **13**, 865–886.

Dawers, N. H., Anders, M. H. & Scholz, C. H. 1993. Growth of normal faults: displacement–length scaling. *Geology* **21**, 1107–1110.

Delaney, P. T. & Pollard, D. D. 1981. Deformation of host rocks and flow of magma during growth of minette dikes and breccia-bearing intrusions near Ship Rock, New Mexico. *U.S. Geol. Surv. Prof. Pap.* **1202**.

Escher, A., Escher, J. C. & Watterson, J. 1975. The reorientation of the Kangamiut Dike Swarm, West Greenland. *Can. J. Earth Sci.* **12**, 158–173.

Gibbs, A. D. 1984. Structural evolution of extensional basin margins. *J. geol. Soc. Lond.* **141**, 609–620.

Gibbs, A. D. 1990. Linked fault families in basin formation. *J. Struct. Geol.* **12**, 795–803.

Gillespie, P. A., Walsh, J. J. & Watterson, J. 1992. Limitations of dimension and displacement data from single faults and the consequences for data analysis and interpretation. *J. Struct. Geol.* **14**, 1157–1172.

Green, D. J., Nicholson, P. S. & Embury, J. D. 1977. Crack shape studies in brittle porous materials. *J. Mater. Sci.* **12**, 987–989.

Hull, D. 1993. Tilting cracks: the evolution of fracture surface topography in brittle solids. *Int. J. Fract.* **62**, 119–138.

Jackson, P. 1987. The corrugation and bifurcation of fault surfaces by cross-slip. *J. Struct. Geol.* **9**, 247–250.

Kerkhof, F. 1973. Wave fractographic investigations of brittle fracture dynamics. In: *Dynamic Crack Propagation* (edited by Sih, G. C.), Noordhof, Leyden, pp. 3–35.

Larsen, P. H. 1988. Relay structures in a Lower Permian basement-involved extension system, East Greenland. *J. Struct. Geol.* **10**, 3–8.

Morley, C. K., Nelson, R. A., Patton, T. L. & Munn, S. G. 1990. Transfer zones in the East African Rift System and their relevance to hydrocarbon exploration in rifts. *Bull. Am. Ass. Petrol. Geol.* **74**, 1234–1253.

Muraoka, H. & Kamata, H. 1983. Displacement distribution along minor fault traces. *J. Struct. Geol.* **5**, 483–495.

Peacock, D. C. P. & Sanderson, D. J. 1991. Displacements, segment linkage and relay ramps in normal fault zones. *J. Struct. Geol.* **13**, 721–733.

Peacock, D. C. P. & Sanderson, D. J. 1994. Geometry and development of relay ramps in normal fault systems. *Bull. Am. Ass. Petrol. Geol.* **78**, 147–165.

Peter, K. 1968. Die Beeinflussung des sproden Bruches durch Materialinhomogenitaten. *Z. angew. Phys.* **25**, 309–313.

Rippon, J. H. 1985. Contoured patterns of the throw and hade of normal faults in the Coal Measures (Westphalian) of north-east Derbyshire. *Proc. Yorks. geol. Soc.* **45**, 147–161.

Rogers, R. D. & Bird, D. K. 1987. Fracture propagation with dike emplacement at the Skaergaard intrusion, East Greenland. *J. Struct. Geol.* **9**, 71–86.

Scholz, C. H. & Cowie, P. A. 1990. Determination of total strain from faulting using slip measurements. *Nature* **346**, 837–839.

Scholz, C. H., Dawers, N. H., Yu, J. Z., Anders, M. H. & Cowie, P. A. 1993. Fault growth and fault scaling laws: preliminary results. *J. geophys. Res.* **98**, 21951–21961.

Segall, P. & Pollard, D. D. 1980. Mechanics of discontinuous faults. *J. geophys. Res.* **85**, 4337–4350.

Stewart, I. S. & Hancock, P. L. 1991. Scales of structural heterogenicity within neotectonic normal fault zones in the Aegean region. *J. Struct. Geol.* **13**, 191–204.

Walsh, J. J. & Watterson, J. 1987. Distributions of cumulative displacement and seismic slip on a single normal fault surface. *J. Struct. Geol.* **9**, 1030–1046.

Walsh, J. J. & Watterson, J. 1989. Displacement gradients on fault surfaces. *J. Struct. Geol.* **11**, 307–316.

Walsh, J. J. & Watterson, J. 1990. New methods of fault projection for coal mine planning. *Proc. Yorks. geol. Soc.* **48**, 209–219.

Walsh, J. J. & Watterson, J. 1991. Geometric and kinematic coherence and scale effects in normal fault systems. In: *The Geometry of Normal Faults* (edited by Roberts, A. M., Yielding, G. & Freeman, B.). *Spec. Publ. geol. Soc. Lond.* **56**, 193–203.

Walsh, J. J., Watterson, J., Childs, C. & Nicol, A. (1995). Ductile strain effects in the analysis of seismic interpretations of normal fault systems. In: *Modern Developments in Structural Interpretation, Validation and Modelling* (edited by Nieuwland, D. A. & Buchanan P. G.). *Spec. Publ. geol. Soc. Lond.* (in press).

Watterson, J., Walsh, J. J., Gillespie, P. A. & Easton, S. In press. Scaling systematics of fault sizes on a large scale range fault map. *J. Struct. Geol.*

Withjack, M. O., Olson, J. & Peterson, E. 1990. Experimental models of extensional forced folds. *Bull. Am. Ass. Petrol. Geol.* **74**, 1038–1054.

Woods, E. P. 1992. Vulcan sub-basin fault styles—implications for hydrocarbon migration and entrapment. *Austr. Petrol. Explor. Ass.* **J32**, 138–158.